Pacific Northwest
NATIONAL LABORATORY

PNNL-30513

Thermoelectric Temperature Measurement of Deforming Solids

October 2020

B. Scott Taysom
Scott Whalen

U.S. DEPARTMENT OF ENERGY

Prepared for the U.S. Department of Energy
under Contract DE-AC05-76RL01830

DISCLAIMER

PACIFIC NORTHWEST NATIONAL LABORATORY
operated by
BATTELLE
for the
UNITED STATES DEPARTMENT OF ENERGY
under Contract DE-AC05-76RL01830

Printed in the United States of America

Available to DOE and DOE contractors from the
Office of Scientific and Technical Information,
P.O. Box 62, Oak Ridge, TN 37831-0062;
ph: (865) 576-8401
fax: (865) 576-5728
email: reports@adonis.osti.gov

Available to the public from the National Technical Information Service
5301 Shawnee Rd., Alexandria, VA 22312
ph: (800) 553-NTIS (6847)
email: orders@ntis.gov <https://www.ntis.gov/about>
Online ordering: http://www.ntis.gov

PNNL-30513

Thermoelectric Temperature Measurement of Deforming Solids

October 2020

B. Scott Taysom
Scott Whalen

Prepared for
the U.S. Department of Energy
under Contract DE-AC05-76RL01830

Pacific Northwest National Laboratory
Richland, Washington 99354

Abstract

Sold phase processing (SPP) utilizes large deformations and elevated but sub-melting temperatures to process materials in an energy-efficient manner to achieve high-performance properties. Studying the fundamental material science and kinetics requires an accurate temperature history of the process, but accurately measuring temperature at the point of deformation is very difficult. This study uses the thermoelectric principle to allow for the direct measurement of a deforming surface by turning the workpieces themselves into the measurement device. By so doing, measured temperatures are closer to the actual deforming interface, more accurate, more responsive, and more reliable than corresponding measurements taken with standard thermocouples.

Keywords: thermoelectricity, temperature

1. Introduction

Solid phase processing (SPP) uses large deformations to process materials at elevated but sub-melting temperature. A key advantage of SPP over many other technologies is that large strains help to induce recrystallization while sub-melting temperatures avoid defects associated with liquation and solidification. SPP includes technologies such as friction stir weld (FSW), friction stir processing (FSP), cold spray, and shear assisted processing and extrusion (ShAPE).

Temperature is one of the most important parameters in SPP and is key to understanding the microstructural mechanisms that occur during SPP. Accurately measuring temperature of a deforming solid is however very difficult. Internal thermocouples and surface measurements are commonly used, each with accompanying benefits and drawbacks.

Thermocouples are often used to measure temperature in solid phase processes such as RFW [1, 2] and FSW [3, 4, 5]. Thermocouples are widely used due to ease of use and price, but have a few limitations. Thermocouples placed in a deforming solid can obtain initially accurate measurements, but moderate strain will destroy the thermocouple [6]. While placing a thermocouple farther away preserves the thermocouple, the measurement is no longer reflective of the deformation zone. Thermocouples can also be placed in a nondeforming adjacent body (such as fixturing or a tool) [7], but again the measured temperature is not representative of the deforming solid.

Infrared is another common temperature measurement method for SPP [8]. Infrared can measure a surface temperature and has near zero risk of sensor destruction unlike thermocouples, but the temperature-dependent emissivity and surface oxidation *must* both be known or compensated for, otherwise the measurement can be wildly off. Determining these properties for a given application can be a research project in and of itself. Furthermore, infrared can only ever be used to measure a surface and never internal temperature. This is less of a concern for application such as RFW of tubes, but becomes nearly impossible for processes such as ShAPE.

The thermometric effect is the underlying principle behind the commercial thermocouple, and has also been used recently to directly measure SPP events. De Backer and Magalhaes have used thermoelectricity to measure the tool-workpiece interface in FSW [9, 10]. Ghodam has used this principle to measure the temperature of a cutting chip in a turning operation [11]. Both of these cases are innovative by directly measuring at the tool surface. Two limitations are that measurements are external and not internal to the deforming solid, and that additional thermometric junctions are often created in the apparatus which results in measurement error.

This study uses the thermoelectric principle to allow for the direct measurement of a deforming surface by turning the workpieces themselves into the measurement device.

2. Thermoelectricity

The thermoelectric or Seebeck effect is a change of electric voltage across a temperature gradient and is the underlying technology behind thermocouples. This was originally discovered in 1774 by Alessandro Volta, and was rediscovered in 1822 by Thomas Seebeck [12]. The Seebeck coefficient can be positive or negative and is a function of temperature as defined in

Equation 1. The Seebeck coefficient is positive for positively charged carriers (p-doped, electron holes), and negative for negatively charged carriers (n-doped, electrons).

$$S(T) = -\Delta V / \Delta T \quad (1)$$

When materials with different Seebeck coefficients are in contact, with both junctions at different temperatures, a thermoelectric circuit is formed. Integrating the temperature-dependent Seebeck coefficient of two materials (S_a and S_b) from the cold to hot junction of one metal and from the hot to cold junction of the other gives the total voltage generated by a thermometric circuit, as shown in Equation 2. The voltage can be used to determine the temperature of one junction if the other junction's temperature is already known, such as by a thermistor. This is how thermocouples work. Since a thermocouple measures the junction temperature, as common misconception is that the voltage is generated across the junction, when in fact the voltage is generated by the thermal gradient within the wire between the location of interest and a reference junction having a known temperature.

$$V = \int_{T_c}^{T_h} -S_a(T)dT + \int_{T_h}^{T_c} -S_b(T)dT = \int_{T_c}^{T_h} (S_b(T) - S_a(T))dT \quad (2)$$

3. Experimental Methods and Materials

3.1. Materials

Copper 110 (99.9% pure copper) and Nickel 200 (min. 99.3% pure nickel) were used for all experiments. 26 AWG wires of these alloys were used both for furnace calibration and as legs connecting the bulk samples to the cold junction. Braided fiberglass insulation was used to insulate the wires from each other and their surroundings.

Measured thermoelectric temperature is an average temperature of all points at a dissimilar junction. Accordingly, a tubular geometry was used for the SPP workpieces to minimize radial temperature differences across the hot deformation interface. Tubular samples were machined to an outer diameter of 31.75 mm (1.25 in) and inner diameter of 25.4 mm (1.00 in). Traditional k-type thermocouples were place 1 mm away from the tip of the nickel specimens to enable comparison to typical measurement methods. The back portion of the tubular samples was coated in alumina in order to electrically isolate them from the toolholder. A picture of the base samples and full setup with samples is shown in Figure 1.

(a)

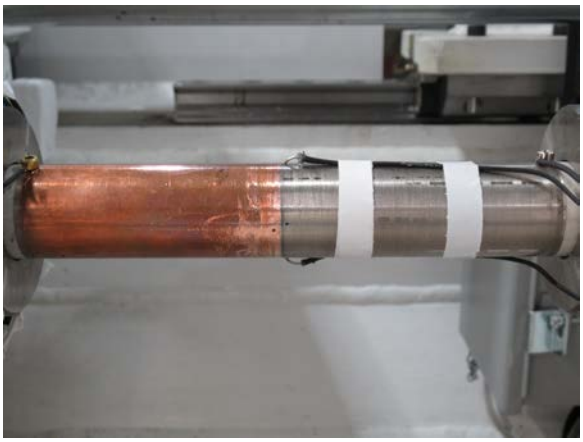

(b)

Figure 1: (a) Copper 100 and Nickel 200 specimens with white alumina coating. (b) Copper and Nickel specimens are mounted in tool holders. A slip ring was used to conduct voltage from the rotating copper workpiece to a stationary terminal block made from Shapal. Additionally, thermocouples were inserted 1 mm away from the tip of the Nickel 200 specimen.

3.2. Measurement and Equipment

A micro-volt and thermocouple data acquisition system was used to measure voltage from the Ni-Cu wire pairs and the k-type thermocouples. This data was used to determine the voltage-temperature relationship and thereby the temperature-dependent Seebeck coefficient. Multiple Ni-Cu wire pairs were calibrated in order to estimate the statistical uncertainly of the calibration.

Knowing the junction temperature is critical for correct thermoelectric measurements. In order to minimize temperature differences between the actual junction and the measurement point, a junction block was made out of Shapal - a technical ceramic similar to AlN - that has a thermal conductivity of 92 W/mK and an electrical resistivity of 1e13 Ω m at 25 C. A picture of this is shown in Figure 2 as it was used both in the furnace and as a cold junction for the furnace calibration and SPP experiments.

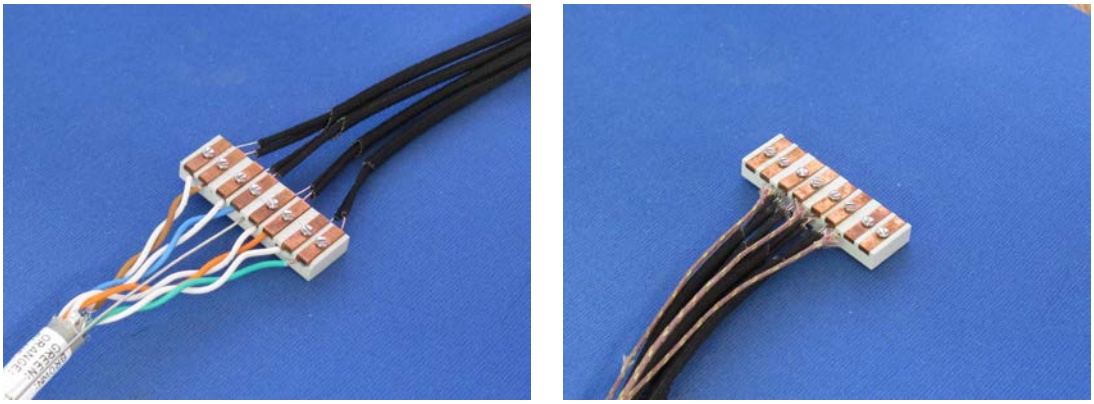

(a) (b)

Figure 2: Picture of Shapal junctions. (a) Cold junction, with shielded twisted pair wires heading to the data acquisition system on the left, with the Ni-Cu wire coming out of the right side, and a single thermocouple inserted into the Shapal block. (b) junction block inserted into the furnace, with four Ni-Cu wire pairs and three standard k-type thermocouples.

A Bond Technologies Shear Assisted Processing and Extrusion (ShAPE) machine was used for all solid-phase deformation experiments. The machine has a 900 kN maximum axial force, 450 rpm maximum spindle speed, and is equipped with B&R IO modules that have 1.06 μV resolution.

3.3. Calibration

The voltage-temperature relationship was determined by furnace calibration. A furnace was ramped from room temperature to about 625 C over 4 hours. The slow ramp rate was chosen to minimize temperature differences. An Omega k-type ”special limits of error” thermocouple (± 1.1 C or 0.4%) was used to measure the cold junction, and three were used for the furnace measurement. Four pairs of Cu-Ni wire were created, with the hot and cold junctions placed next to the sets of k-type thermocouples in a Shapal junction block. Shielded twisted-pair copper wire was used to connect the cold junction to the Pico-TC8 micro-volt reader, which collected data at 1 Hz. Calibration data was filtered using a mild first-order butterworth filter which reduced noise in the signal without affecting longer term trends.

3.4. Solid State Processing

Tubular samples were inserted into tool holders mounted onto the spindle and tailstock of the ShAPE machine. The spindle was rotated at a constant speed while the tailstock pushed towards the rotating spindle specimen. The parameters for each experiment are shown in Table 1. Sensor feedback was acquired at 100 Hz during solid state processing.

Table 1: Solid State Processing Experimental Matrix

Trial Num.	Axial Speed	Upset	Spindle Speed	Revolutions	Advance per Revolution
1	0.1 mm/s	2 mm	60 rpm	20 rev	5 μm
2	0.1 mm/s	2 mm	240 rpm	80 rev	1.25 μm
3	0.4 mm/s	8 mm	60 rpm	20 rev	20 μm
4	0.4 mm/s	8 mm	240 rpm	80 rev	5 μm

3.5. Microstructure Analysis

After solid state processing, the Ni-Cu interface was parted from the workpiece, sliced longitudinally, mounted in epoxy pucks, and polished to a 0.05μm finish using colloidal silica for the final step. Pucks were coated with a thin layer to platinum to avoid charging of the epoxy. An SEM was used to analyze the chemical composition and microstructure of processed pieces.

4. Results and Discussion

4.1. Temperature-Voltage Relationship

Across the four calibration runs, average difference in temperature between each of the three wire pairs was about 1.3 C. The voltage-temperature relationship from the furnace calibration is shown in Figure 3. An equation relating electrical potential (in mV) to temperature (in C), relative to a cold junction temperature of 0 C, is given in Equation 3. Over the range of 25 C to 625 C, the average absolute error between the data and fit equation is 31 μV or about 1.3 C.

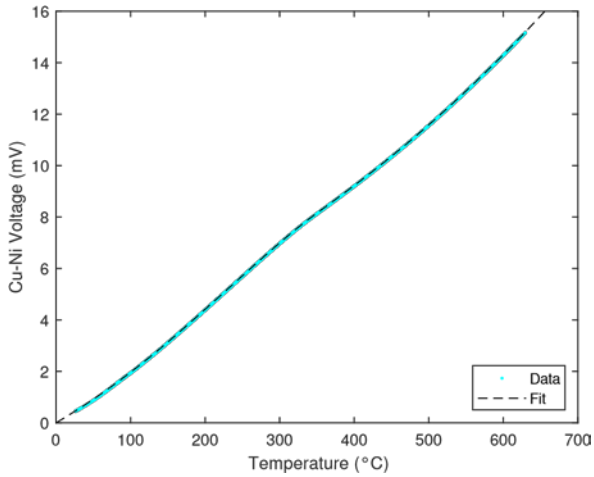

Figure 3: Voltage of the Cu 110 - Ni 200 wire pairs from 25 C to 625 C (cyan), with a quadratic fit curve (dashed line).

$$V_{Cu-Ni}(T) = 1.327 \times 10^{-10}\,T^4 - 1.643 \times 10^{-7}\,T^3 + 6.677 \times 10^{-5}\,T^2 + 1.42 \times 10^{-2}\,T \quad (3)$$

The temperature-dependent Seebeck coefficient of Copper 110 with reference to Nickel 200 is calculated as the derivative of voltage with respect to temperature, and is shown in Figure 4. This is also compared to the relative Seebeck coefficient of pure copper relative to pure nickel as determined by others by subtracting their findings on nickel [13, 14, 15] from the linear Seebeck coefficient of copper [13]. It is hypothesized that differences in measurement are due to experiment apparatus setup and slight differences in chemistry between pure Cu and Ni to Cu 110 and Ni 200.

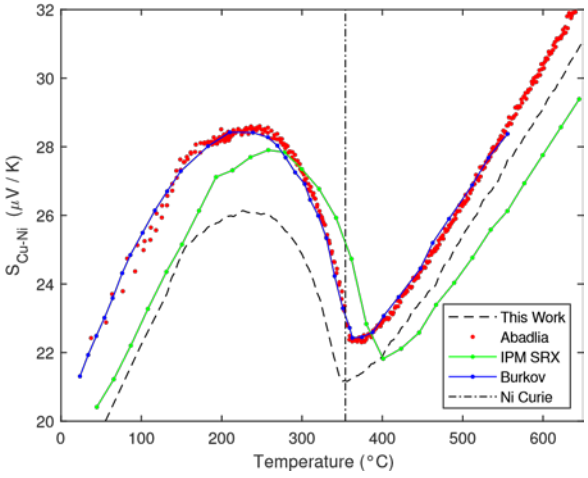

Figure 4: Seebeck coefficient of Cu 110 relative to Ni 200, along with data from others for pure copper [13] relative to pure nickel [13, 14, 15]. The curie temperature of Ni at 354 C is also shown, which roughly corresponds to a discontinuous derivative in the Seebeck coefficient at 351 C for the present work, 361 C for Adablia and Burkov, and an estimated 395 C for IMP SRX.

4.2. Solid State Processing

Time series data for each of the four runs is shown below in Figure 5 a-d.

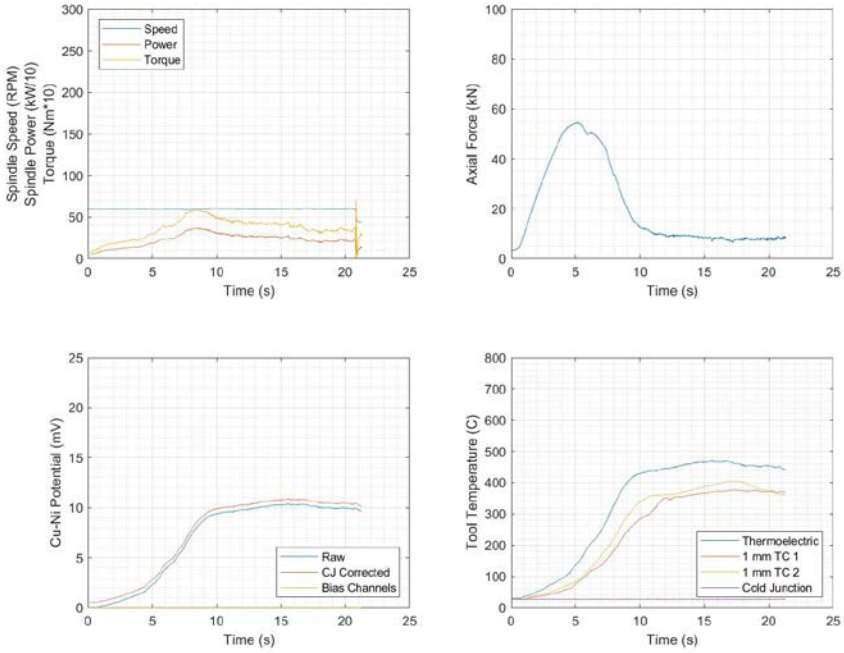

(a)

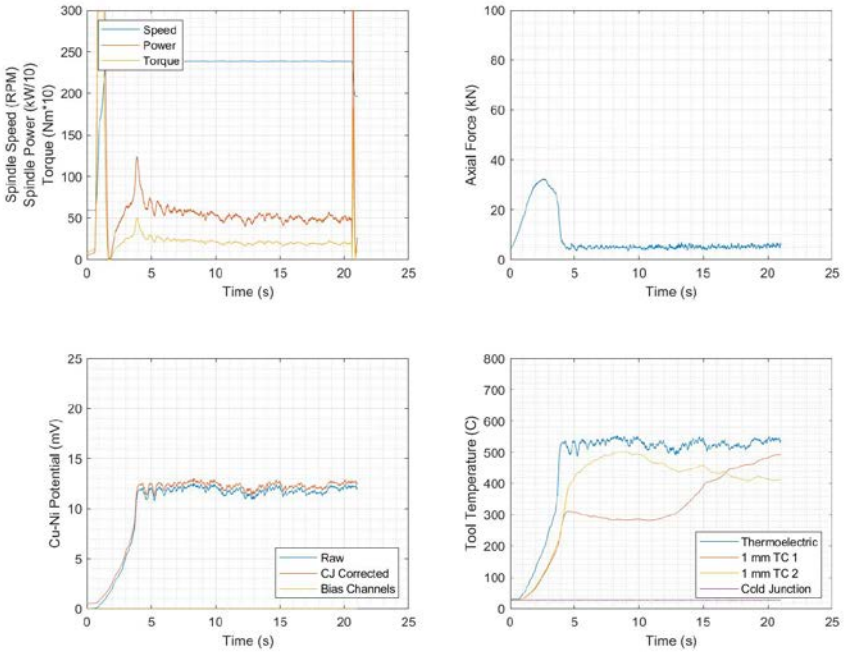

(b)

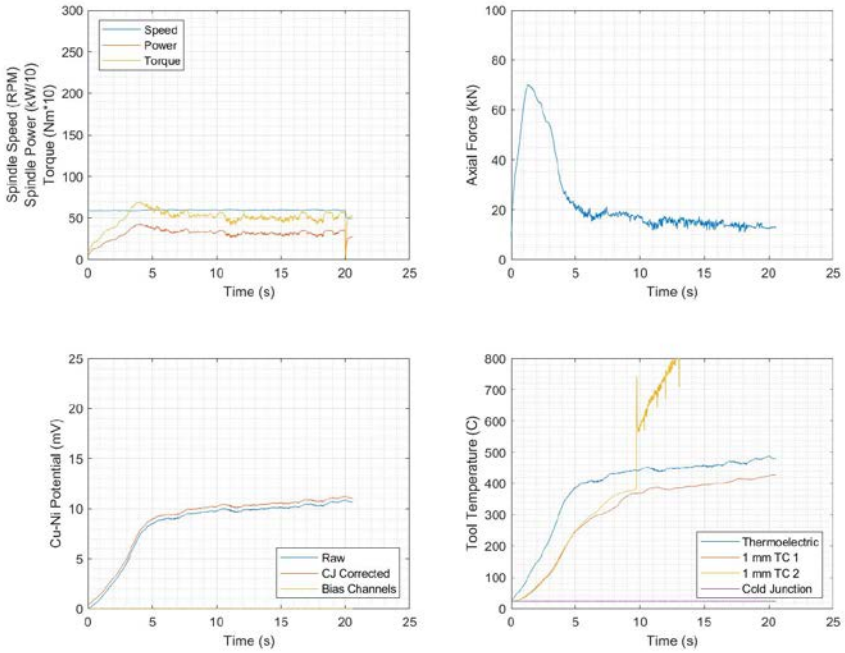

(c)

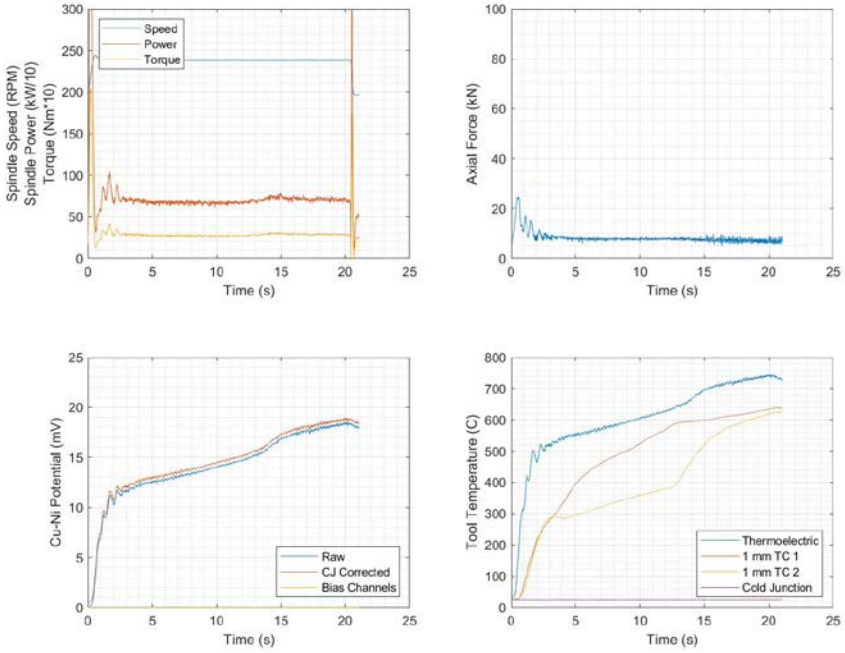

(d)

Figure 5: Time series data including: spindle power, speed, and torque; axial force; measured and cold-junction compensated voltage; temperatures from thermocouples and from Cu-Ni wire pairs. (a) Trial #1, (b) trial #2, (c) trail #3, and (d) trial #4.

From the time series data, the thermoelectric measurement appears to be more reliable. This is because it is easy for a thermocouple to become dislodged or damaged when placed close to the region of deformation. This is seen in Figure 5 b-d where a k-type thermocouple has an issue and reports incorrect data mid-way through the run, while the thermoelectric measurement is steady throughout.

The thermoelectric measurement also gives a truer reading than the k-type thermocouples. This can be seen by the fact that even though the k-type thermocouples are only 1 mm away from the interface, they have a 60-100 C lower temperature reading compared to the thermoelectric measurements.

Another difference between the thermoelectric and thermocouple measurement can be seen in Figure 6, which is a portion of the data at the end of trial #3. Here, the spindle and workpiece experienced power fluctuations although the cause of these is unknown. Importantly, there are three segments that act as an effective “step test”, allowing an analysis of the response dynamics of the system. The thermoelectric measurement has a near-zero measurement delay, whereas the thermocouple takes ~0.2 – 0.5 s to start showing a response to the power change.

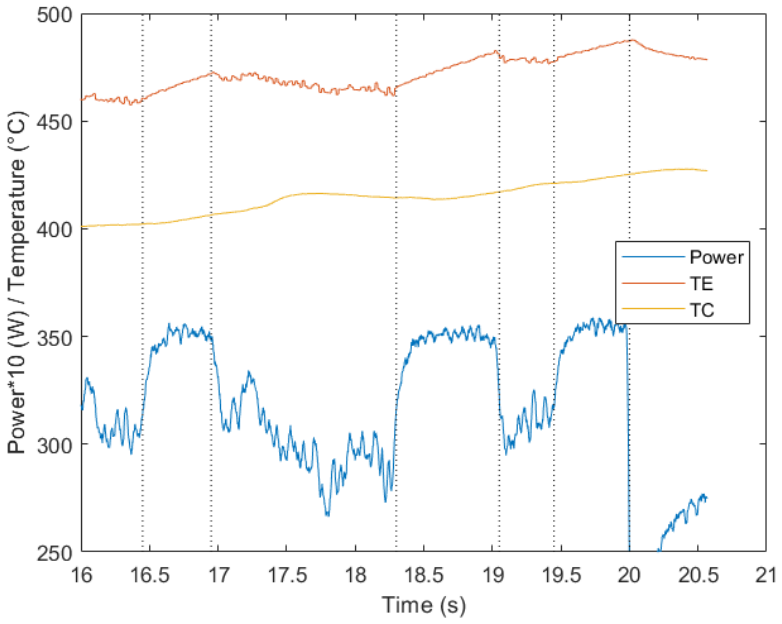

(d)

Figure 6: Response of the thermoelectric and standard thermocouples due to a fluctuating spindle power. The thermoelectric interface measurement responds much quicker than does a standard thermocouple 1 mm away from the interface.

4.3. Microscopy

Microscopy was performed on the processed tips of trials 1 and 2. After processing, the tips of the workpiece naturally broke away from each other, leaving a macro deformed copper side, with the nickel shown no macro deformation with some copper build up on the former interface. Micrographs of the remaining Cu-Ni interface are shown in Figure 7.

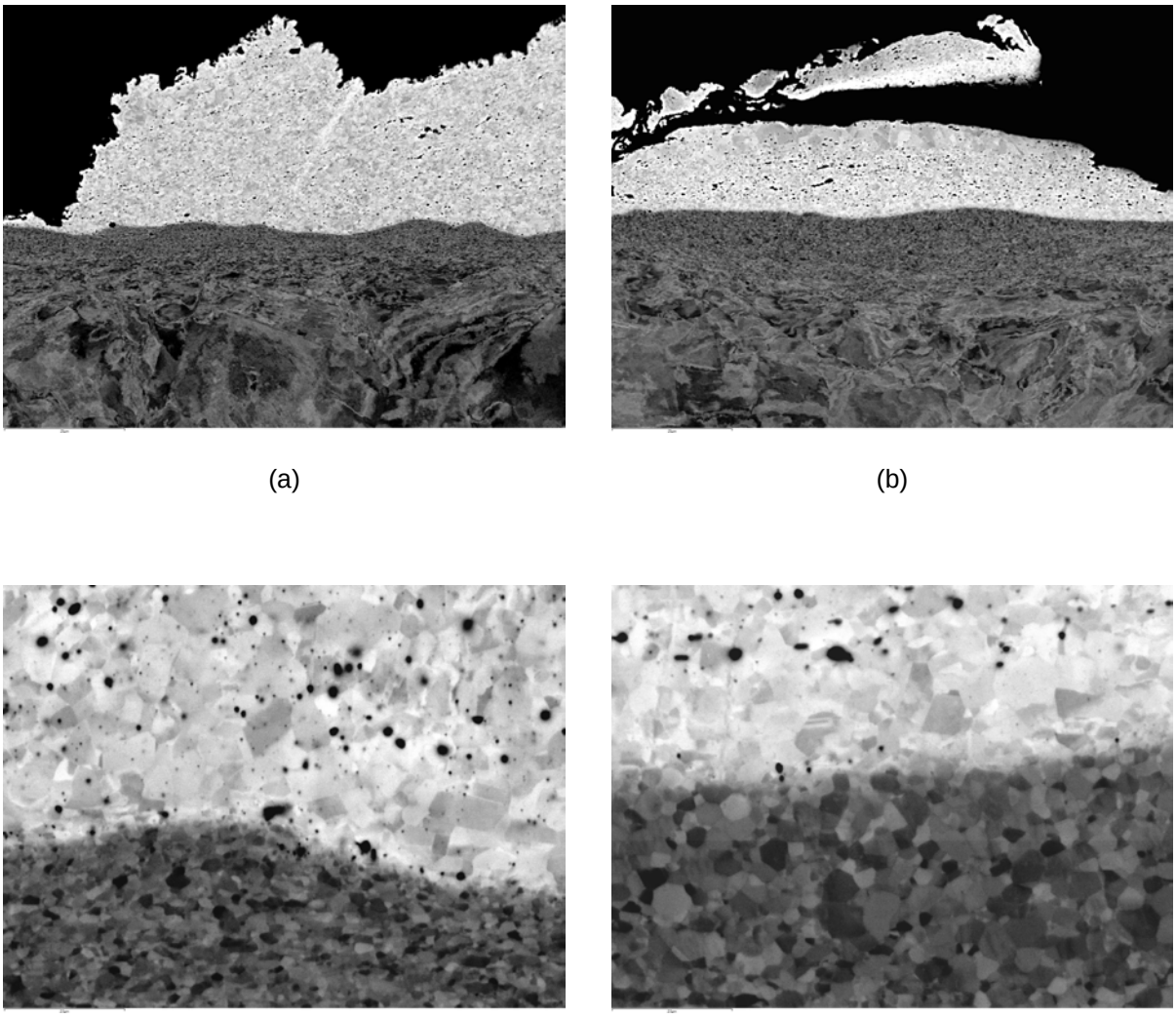

(a) (b)

(c) (d)

Figure 7: Micrographs of the Cu Ni interface for trials 1 and 2. The Cu is on the top of each image in a nearly white color, and the Ni is on the bottom in dark grey. Trial 1 is shown at magnifications of 1,000x (a) and 10,000x (c), and trial 2 is shown at magnifications of 1,000c (b) and 10,000x (d).

Both samples show significant sub-surface deformation as evidenced the wavy strain contouring in the Ni. Trial 1 had an average steady state temperature of about 450 C, compared to 540 C

for trial 2. The higher temperature provides the necessary energy for recrystallization. As a result, trial 1 had a recrystallized layer that was 10 μm thick, compared to 15 μm thick for trial 2. Limited diffusion may have occurred at the interface based upon a subtle gradient between the Cu and Ni interface in Figure 7c- d, although more detailed analysis is be needed to confirm for refute this.

5. Conclusions and Future Work

The thermoelectric effect can be used to take direct measurements of the interface of two dissimilar deforming solids. Calibration results suggests that an absolute accuracy of 1-2 C is achievable with this setup. The thermoelectric measurement of a deforming solid was much more responsive than standard thermocouples, with no apparent time delay. Not only that, but even though the thermocouples were only 1 mm away from the interface, the thermocouple temperature was about 60-100 C lower than the thermoelectric measurement even at steady state.

The work is immediately applicable to measuring applications such as rotary friction welding of dissimilar alloys. Other applications to this method include extrusion technologies like ShAPE. Another very promising research area is tribology, where the deformation heat must be measured, but the deforming depth is very thin and fully covered by a harder deforming body, thus making a classical thermocouple or infrared measurement difficult.

References

[1] B. S. Taysom, C. D. Sorensen, Controlling martensite and pearlite formation with cooling rate and temperature control in rotary friction welding, International Journal of Machine Tools and Manufacture 150. doi:10.1016/j.ijmachtools.2019.103512.

[2] W. Li, A. Vairis, M. Preuss, T. Ma, Linear and rotary friction welding review, International Materials Reviews 61 (2) (2016) 71–100. doi:10.1080/09506608.2015.1109214.

[3] K. Ross, C. D. Sorensen, Advances in temperature control for FSP, in: Friction Stir Welding and Processing VII, John Wiley & Sons, Inc., 2013, pp. 301–310. doi:10.1007/978-3-319-48108-1.
URL http://www.scopus.com/inward/record.url?eid=2-s2.0-84876443078&partnerID=40&md5=d45693b1d90b7

[4] L. Cederqvist, O. Garpinger, T. H¨agglund, Reliable Sealing of Copper Canisters Through Cascaded, in: R. Mishra, M. W. Mahoney, Y. Sato, Y. Hovanski, R. Verma (Eds.), Friction stir welding and processing VI, Friction Stir Welding and Processing VI, John Wiley & Sons, Inc., Hoboken, NJ, 2011, pp. 51–58.

[5] R. S. Mishra, M. W. Mahoney, Y. Sato, Y. Hovanski, Friction stir welding and processing VIII, in: Friction Stir Welding and Processing VIII, Friction Stir Welding and Processing VII, John Wiley & Sons, 2016, pp. 1–300. doi:10.1007/978-3-319-48173-9.
URL http://www.scopus.com/inward/record.url?eid=2-s2.0-84876451017&partnerID=40&md5=921c76534496c

[6] T. W. Nelson, S. A. Rose, Controlling hard zone formation in friction stir processed HSLA steel, Journal of Materials Processing Technology 231 (2016) 66–74. doi:10.1016/j.jmatprotec.2015.12.013.

[7] L. Cederqvist, O. Garpinger, T. H¨agglund, A. Robertsson, Cascade control of the friction stir welding process to seal canisters for spent nuclear fuel, Control Engineering Practice 20 (1) (2012) 35–48.

[8] S. Celik, I. Ersozlu, Investigation of the mechanical properties and microstructure of friction welded joints between AISI 4140 and AISI 1050 steels, Materials and Design 30 (4) (2009) 970–976. doi:10.1016/j.matdes.2008.06.070.

[9] J. De Backer, G. Bolmsjo, A.-K. Christiansson, Temperature control of robotic friction stir welding using the thermoelectric effect, International Journal of Advanced Manufacturing Technology 70 (1-4) (2014) 375–383. doi:10.1007/s00170-013-5279-0.

[10] A. Magalh˜aes, Thermo-electric temperature measurements in friction stir welding – Towards feedbackcontrol of temperature, Ph.D. thesis (2016).

[11] S. D. Ghodam, Temperature Measurement of a Cutting Tool in Turning Process By Using Tool Work Thermocouple, International Journal of Research in Engineering and Technology 03 (04) (2014) 831– 835. doi:10.15623/ijret.2014.0304147.

[12] T. J. Seebeck, Ueber die magnetische Polarisation der Metalle und Erze durch Temperatur-Differenz, Annalen der Physik 82 (2) (1826) 133–160. doi:10.1002/andp.18260820202.

[13] L. Abadlia, F. Gasser, K. Khalouk, M. Mayoufi, J. G. Gasser, New experimental methodology, setup and LabView program for accurate absolute thermoelectric power and electrical resistivity measurements between 25 and 1600 K: Application to pure copper, platinum, tungsten, and nickel at very high temperatures, Review of Scientific Instruments 85 (9). doi:10.1063/1.4896046.

[14] A. T. Burkov, A. Heinrich, P. P. Konstantinov, T. Nakama, K. Yagasaki, Experimental set-up for thermopower and resistivity measurements at 100-1300 K, Measurement Science and Technology 12 (3) (2001) 264–272. doi:10.1088/0957-0233/12/3/304.

[15] J. D. K¨onig, K. Bartholom´e, M. J¨agle, H. B¨ottner, Overview of Fraunhofer IPM Activities in High Temperature Bulk Materials and Device Development, in: 2nd Thermoelectrics Applications Workshop 2011, 2011, pp. 1–34.
URL https://www1.eere.energy.gov/vehiclesandfuels/pdfs/thermoelectrics app 2011/tuesday/konig.pdf

Pacific Northwest National Laboratory

902 Battelle Boulevard
P.O. Box 999
Richland, WA 99354
1-888-375-PNNL (7665)

www.pnnl.gov